



Carbon coated nitrogen doped P25 for the photocatalytic removal of organic pollutants under solar and low energy visible light irradiations

W.I. Nawawi, M.A. Nawi*

Photocatalysis Laboratory, School of Chemical Sciences, Universiti Sains Malaysia, Pulau Pinang, Malaysia



ARTICLE INFO

Article history:

Received 5 August 2013

Received in revised form

18 November 2013

Accepted 26 November 2013

Available online 6 December 2013

Keywords:

Degussa P25

Urea

Reactive red 4

Methylene blue

Phenol

ABSTRACT

The commercially available TiO₂ Degussa P25 was modified using a simple technique to produce a visible light active carbon (C) coated and nitrogen (N) doped P25. The modified photocatalyst was prepared by mechanical mixing of P25 powder with various amount of urea and followed by thermal heating under semi-closed reactor at different temperatures. The results showed that a layer of carbon graphite was deposited on the surface of P25 and N atoms were incorporated into the lattice of the nano-scaled photocatalyst. It was observed that the UV-Vis spectra of the modified photocatalyst exhibited red shift to the visible region as compared to that of the pristine P25, implying the decreased of band gap energy for the modified photocatalyst. Moreover, the modified photocatalyst was found to yield efficient photocatalytic degradations of the RR4, MB and phenol pollutants under visible light and solar light irradiations.

© 2013 Elsevier B.V. All rights reserved.

1. Introduction

The various advantages of titanium dioxide (TiO₂) as a photocatalyst for effective photocatalytic removal of organic pollutants in water effluents have received great attention from many researchers [1]. Unfortunately, the use of TiO₂ technology is limited by its wide band gap energy ($E_g = 3.2$ eV) which requires UV light irradiation for its photocatalytic activity. The UV light of the sun only accounts for a small fraction (3–5%) of the sun's light spectrum compared to visible light [2]. Thus any attempt of making TiO₂ to absorb visible light will have a profound positive effect on its photocatalytic applications in environmental remediation. For this purpose, various efforts have been directed towards the development of visible-light responsive TiO₂ materials.

The modification of TiO₂ towards narrowing its band gap allows the utilization of a wider fraction of visible light for the production of charge carriers. Incorporation of metal ions like Pt, Au, Ag, Cu, Fe and nonmetals such as C, N, S, F and P into TiO₂ have been proposed in order to improve its photocatalytic activity [3–13]. Nitrogen and carbon have been widely used for modification of TiO₂ due to their capabilities in narrowing the photocatalyst's band gap which led to better photo-response and subsequently enhanced photocatalytic activity [3–5]. Interestingly, simultaneous co-doped TiO₂ with C and N was reported to show a synergistic effect on its

photocatalytic activities [10–12]. Chen et al. [10] prepared C, N co-doped TiO₂ using the sol-gel method where the product exhibited higher photocatalytic activity under visible light as compared to either C-doped TiO₂ or N-doped TiO₂. They attributed this phenomenon to the enhanced adsorption of carbonate species on the surface of the C, N co-doped TiO₂ where the visible light photoactivity was induced by N-doping into the TiO₂ lattice. Another interesting modification of TiO₂ involved the preparation of a composite of N doped TiO₂–Al₂O₃. In this work, Li et al. [14] had proven that N element can be doped into the lattice of TiO₂ using urea and nitrate as the N precursor in the presence of aqueous Al₂O₃ solution at the calcination temperature of 300 °C. However, they also proved that C was not detected within the modified catalyst. The product was observed to be 43.6 times faster than that of pristine P25 TiO₂ in the photocatalytic degradation of methyl orange. The high visible-light photocatalytic activity was attributed to synthetic effects between amorphous Al₂O₃ and TiO₂, low recombination efficiency of photo-excited electrons and holes, N-doping, and a large specific surface area.

According to Park et al. [4] C doped has been interpreted either as an anion that replaces oxygen substitutionally in the lattice to produce carbides with Ti-C bond, or as a cation that occupy interstitial lattice site to produce carbonates with Ti-O-C bond. The presence of C without the detection of Ti-C or Ti-O-C bonding systems normally means that C is coated on TiO₂. Wang et al. [15] produced C-sensitized N-doped TiO₂ via a facile sol-gel method using titanium butoxide as both titanium precursor and carbon source, and nitric acid as nitrogen source. The incorporated

* Corresponding author. Tel.: +6046534031; fax: +6046574854.

E-mail address: masri@usm.my (M.A. Nawi).

carbonaceous species could serve as photosensitizer, while the nitrogen doping could lead to the remarkable red shift of absorption edge of C/N-TiO₂. The C/N-TiO₂ exhibited the highest photocatalytic activity for sulfanilamide (SNM) degradation under irradiation of visible-light-emitting diode (vis-LED). A simple preparation of N-doped and S, N-doped P25 was done by Herrera et al. [16] using a simple mechanical mixing of P25 with urea as N precursor and thiourea as N, S precursor annealed under open atmosphere. It was found that S, N doped P25 showed better photocatalytic activity than N doped P25 in the photocatalytic degradation of phenol and *E. coli* under visible light irradiation.

The main objective of this study is to produce C coated, N doped P25 by a simple technique which engages the mechanical mixing of P25 with urea where urea serves as both carbon and nitrogen precursor. The preparation of C coated, N doped P25 was done according to the method applied by Herrera et al. [16] with several modifications whereby the mixture of photocatalyst powder and urea was heated under semi-closed reactor to produce C coated and N doped P25. The modified photocatalyst was characterized by HRTEM, XPS, BET, UV-Vis DRS, PL and its photocatalytic activities were tested by photocatalytic degradation of cationic RR4 dye, anionic MB dye and phenol under solar and low energy visible light fluorescent lamp.

2. Experimental

2.1. Material

TiO₂ Degussa P25 powder was used as the starting material in the preparation of C coated, N doped P25. Urea from Fluka (chemical formula: NH₂CONH₂, MW: 60.06 g mol⁻¹) was used as the C and N precursor. Reactive red 4 (RR4) dye or commonly known as Cibacron Brilliant Red (Colour Index Number: 18105, chemical formula: C₃₂H₂₃ClN₈Na₄O₁₄S₄, MW: 995.23 g mol⁻¹, λ_{max} : 517 nm) with 50% dye content was provided by Aldrich Chemical. Methylene blue (MB) dye (c.a. 98%, colour index number: 52015, chemical formula: C₁₆H₁₈ClN₃S₂H₂O) was purchased from Unilab while phenol (99.5%) was obtained from Scharlau. Ultra pure water (18.2 MΩ cm⁻¹) was used to prepare all solutions in this work. Table 1 provides a summary of organic pollutants models used in this work.

2.2. Preparation of C coated, N doped P25 samples

C coated, N doped P25 samples were prepared by thermal heating process using a custom made semi-closed reactor placed in a muffle furnace. The overall experimental set-up is shown in Fig. 1. For a typical preparation, 3 g of TiO₂ (P25) was mixed with various amount of urea in powder form by mechanical mixing process for 5 min. The mixed powder was then placed into a conical flask in the semi-closed reactor. The reactor was then placed into a muffle furnace under the heating temperature ranging from 300 to 500 °C under normal atmospheric condition for 2 h. The sample was then taken out from the muffle furnace and cooled down to room temperature. The products were cleaned by sonicating the sample in a 0.1 N HCl and centrifuged to isolate the contamination. The modified sample was finally washed thoroughly using distilled water under 0.45 µm cellulose nitrate membrane filter to yield a yellowish solid of pure C coated, N doped P25 sample.

The labeling of each sample was based on the amount of urea added and the heating temperature used. The preparation conditions of C coated, N doped P25 samples are listed in Table 2 (column 1 and 2). A sample labeled as PU1-350 means C coated, N doped P25 prepared from the doping of 1 g of urea and calcined at 350 °C (see Table 2, column 1).

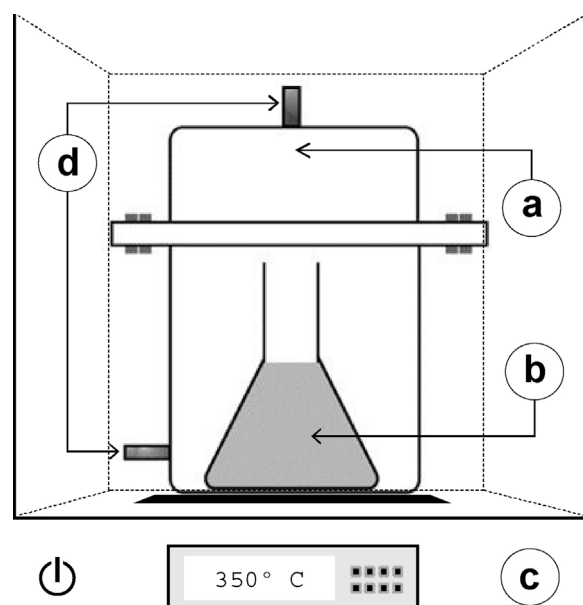


Fig. 1. The experimental setup for preparing C coated N doped P25 using the calcinations process. (a) Semi-closed reactor, (b) sample (c) muffle furnace and (d) ventilation tubes.

2.3. Characterization of C coated N doped P25

The percentage of C and N in TiO₂ (P25) was determined by elemental analyzer CHNS-O (LECO-938) with 0.001% detection limit. UV-Vis diffuse reflectance spectra were recorded using the UV/Vis spectrometer model Lambda 35, Perkin Elmer. High resolution transmission electron microscopy (HRTEM) analysis was performed using FEI Tecnai 20 TEM. BET surface areas was obtained via Micromeritics ASAP 2000 gas adsorption surface analyzer, zeta potentials for photocatalysts in aqueous solutions were measured using Zetasizer Nano Series ZS analyzer model Malvern Nano ZS. Photoluminescent spectrometer model Joblin Yvon HR800 UV was used to obtain the photoluminescence spectra (PL) of the samples while X-ray photoelectron spectroscopy (XPS) spectra were recorded using Omicron Nanotechnology (ELS5000) system using Al K α radiation at a base pressure below 5.5×10^{-9} Torr.

2.4. Adsorption study

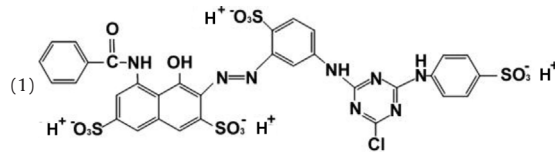
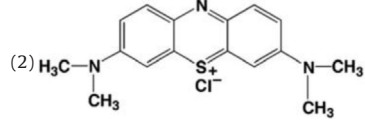
For adsorption study, experiments were conducted in the dark. In each test, 0.024 g of photocatalyst samples were added into a 20 mL solution of 30, 12 and 10 mg L⁻¹ of anionic RR4 dye, cationic MB dye and phenol solutions, respectively, to form suspensions. Those suspensions were then poured into a custom made glass cell with dimension 50 × 10 × 80 (L × B × H) mm and aerated in the dark. Samples were taken at 15 min interval for up to 1 h, filtered with 0.45 µm syringe filter. The decolorization degree of RR4 and MB dye was determined by using a spectrophotometer HACH DR/2000 at wavelength 517 and 661 nm, respectively, while a Shimadzu LC-10 ATVP high performance liquid chromatography (HPLC) with a C18 column was used for detecting phenol where its UV detector was set at 220 nm with 60: 40 methanol-water mixture as the mobile phase.

2.5. Photocatalytic study

In each test, 0.024 g of photocatalyst sample was added into a 20 mL of 30, 12 and 10 mg L⁻¹ of anionic RR4 dye, cationic MB dye and phenol solutions, respectively, to form suspensions and were then individually poured into a glass cell and irradiated under

Table 1

Summary of organic pollutants.

Chemical structures and organic pollutant	Properties		
	Chemical formula	Molecular weight (g mol ⁻¹)	Absorption max (nm)
(1) 	C ₃₂ H ₂₃ ClN ₈ Na ₄ O ₁₄ S ₄	995.23	517 nm
Reactive Red 4 dye (RR4)			
(2) 	C ₁₆ H ₁₈ ClN ₃ S·2H ₂ O	319.85	661 nm
Methylene blue dye (MB)			
(3) 	C ₆ H ₆ O	94.11	220 nm
Phenol			

continuous aeration with a low energy Phillips 45-W compact fluorescent lamp (source no.1) and solar (source no.2) light. In another experiment, a UV filter Contact L6 was placed right in front of the 45-W fluorescent lamp to filter the UV irradiance leakage thus providing a visible light source (source no. 3). The UV detector Radiometer (Solar light co. PMA 2100) connected with a UV-A, UV-B detector (range from 260 to 400 nm) and PAR Quantum Light Sensor detector (range from 401 to 700 nm) was used to determine the UV and visible light irradiance of each source, respectively. The experiments under solar light were carried out on a sunny day from 11.00 am to 3.00 pm. The experimental set up for the

lamp, solar and visible light irradiation (source no.1, 2 and 3) are shown in Fig. 2. An aquarium pump model NS 7200 was used as the aeration source. A direct reading air flowmeter (Gilmont) was used to determine the aeration rate supply to the reactor. Samples were taken at a specific time interval until almost complete decolourisation was attained. The degradation degree of RR4 and MB and phenol was determined by using a HACH DR/2000 spectrophotometer and HPLC as described in the previous section.

For total organic carbon (TOC) analysis, three 10 mL portions of each treated solutions were taken and transferred into vials. The

Table 2

Experimental conditions and results of the modified TiO₂. Pseudo first order rate constants (k) for the degradation of 30 mg L⁻¹ RR4 anionic dye were obtained under low energy Phillips 45 watts fluorescent light irradiation with residual UV leakage of 3.5 W m⁻².

TiO ₂ samples	Temp (°C)	Urea (g)	C (wt%)	N (wt%)	S.Area (m ² g ⁻¹)	Rate const. (k min ⁻¹)		
						RR4	MB	phenol
P25	30	0	0.00	0.00	49.25	0.088	0.021	0.018
P25	350	0	0.00	0.00	49.21	0.057	0.019	0.017
PU0.5–300	300	0.5	0.72	1.98		0.038		
PU0.5–350	350	0.5	0.75	1.92		0.053	0.021	0.017
PU0.5–400	400	0.5	0.74	1.91		0.061		
PU0.5–450	450	0.5	0.73	1.84		0.044		
PU0.5–500	500	0.5	0.72	1.75		0.024		
PU1–300	300	1.0	1.37	2.25		0.052		
PU1–350 ^a	350	1.0	1.39	2.24	34.54	0.158	0.038	0.026
PU1–400	400	1.0	1.37	2.22		0.132		
PU1–450	450	1.0	1.38	2.19		0.051		
PU1–500	500	1.0	1.39	2.05		0.050		
PU1.5–300	300	1.5	2.03	3.77		0.048		
PU1.5–350	350	1.5	2.01	3.72		0.148	0.034	0.024
PU1.5–400	400	1.5	2.03	3.61		0.128		
PU1.5–450	450	1.5	1.95	3.54		0.041		
PU1.5–500	500	1.5	2.04	3.47		0.034		
PU2–300	300	2.0	2.48	4.88		0.047		
PU2–350	350	2.0	2.42	4.68		0.117	0.031	0.022
PU2–400	400	2.0	2.47	4.51		0.100		
PU2–450	450	2.0	2.42	4.38		0.034		
PU2–500	500	2.0	2.44	4.20		0.020		
PU2.5–300	300	2.5	2.91	5.81		0.047		
PU2.5–350	350	2.5	2.86	5.67		0.117	0.028	0.020
PU2.5–400	400	2.5	2.89	5.58		0.100		
PU2.5–450	450	2.5	2.85	5.50		0.034		
PU2.5–500	500	2.5	2.87	5.31		0.020		
PU5–350	350	5.0	4.13	8.64		0.047	0.013	0.011

^a Labeling of samples such as PU1–350 means P25 doped with 1 g Urea heated at 350 °C to produce C-coated N-doped TiO₂ samples.

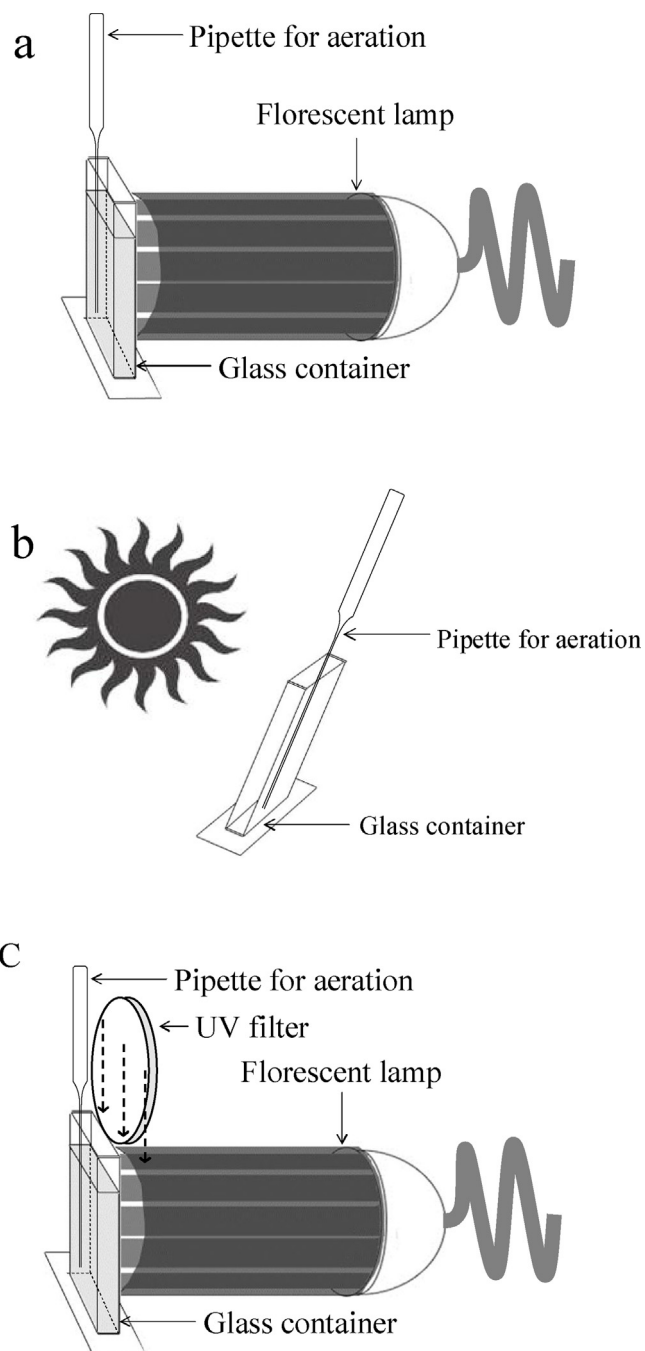


Fig. 2. The photocatalytic experimental set up for the degradation of anionic RR4 dye, cationic MB dye and phenol where (a) under a 45-W fluorescent lamp (UV irradiance leakage of 3.5 W m^{-2} , Visible light: 311 W m^{-2}), (b) under solar irradiation (UV: 22 W m^{-2} , Visible light: 430 W m^{-2}), and (c) under visible light irradiation (UV: 0.0 W m^{-2} , Visible light: 256 W m^{-2}).

amounts of TOC of the treated solutions were then evaluated by a total carbon analyzer (Shimadzu TOC 5000).

3. Results and discussion

3.1. Characteristics

3.1.1. CHN and BET analyses

C and N content of the modified photocatalyst samples prepared at various heating temperatures and dosages of urea are summarized in Table 2 (column 4 and 5). For control purposes, a P25 sample

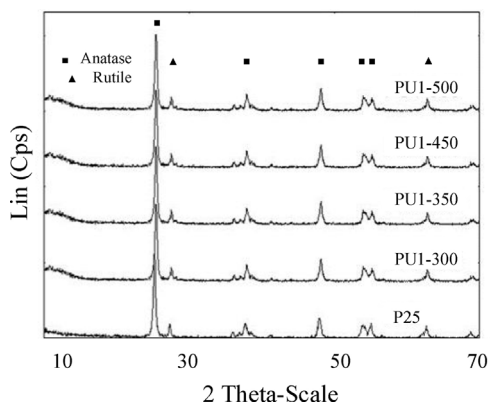


Fig. 3. XRD patterns of the pristine P25 and C coated N doped P25 samples prepared using 0.6 g urea dosage at different calcination temperatures.

in its pristine form was also heated at 350°C where no detection of C and N was observed. As shown in Table 2, the C and N contents of the product depended mainly on the amount of urea added into the P25 samples. The selected range of temperatures used for this study (300 to 500°C) did not significantly affect the C content of the products which was in contrast to other published works where they found that increasing calcination temperatures ($>700^\circ\text{C}$) decreased the amount of C [17,18]. The probable reason for this observation was due to the relatively low temperature usage during the sample preparation. On the other hand, the amount of N seems to be slightly reduced with increasing calcination temperatures. According to Sato et al. [19], N content decreased even at temperature as low as 400°C . They also reported that the decreasing amount of N was due to the sintering effect at 400°C .

Table 2 also provides the BET surface areas for PU1-350 and P25 samples. As observed by a number of workers [20,21], C coated TiO_2 and N doped P25 normally have smaller BET surface areas as compared to the pristine P25. The additional C and N elements in TiO_2 should result in the increment of particle size of the C coated N doped P25. The decreased in surface area was said to be due to the sintering effect [22]. In line with others [22–24], the surface area of PU1-350 was 30% smaller compared with pristine P25.

3.1.2. XRD spectra

Fig. 3 shows the XRD patterns for pristine and C coated N doped P25 at various temperatures. As observed by others [22,23,25], no phase transformation occurred for the calcined samples even at 500°C . In fact Zhang et al. [23] observed the occurrence of phase transformation of C coated TiO_2 only when the calcining temperature was at 900°C while Hsu et al. [22] observed the phase transformation for N doped TiO_2 to occur at 800°C . In our case, the crystallinity of C coated, N doped P25 was not affected since the operation temperature was carried out within the range of 300 to 500°C which was too low for phase transformation of P25 to occur.

3.1.3. UV-Vis spectra

Fig. 4 shows the UV-Vis diffuse reflectance spectra of C coated N doped P25 and pristine P25. As expected, the pristine P25 sample exhibited absorption only in the UV region, whereas the optical response of C coated N doped P25 had absorption both in the UV and visible region. The visible light absorption for C coated N doped P25 is associated with the doped nitrogen which can introduce an impurity level between the valence and conduction band of TiO_2 or narrow the band gap by mixing the N 2p and O 2p states [3,26]. Kubelka-Munk function was used to estimate the band gap energy of the prepared samples by plotting $(\alpha h\nu)^{1/2}$ versus energy of light (see Figs. 5 and 3b). Results indicated that the band gap energies of pristine P25 were 3.1 eV which was equal to the band gap energy

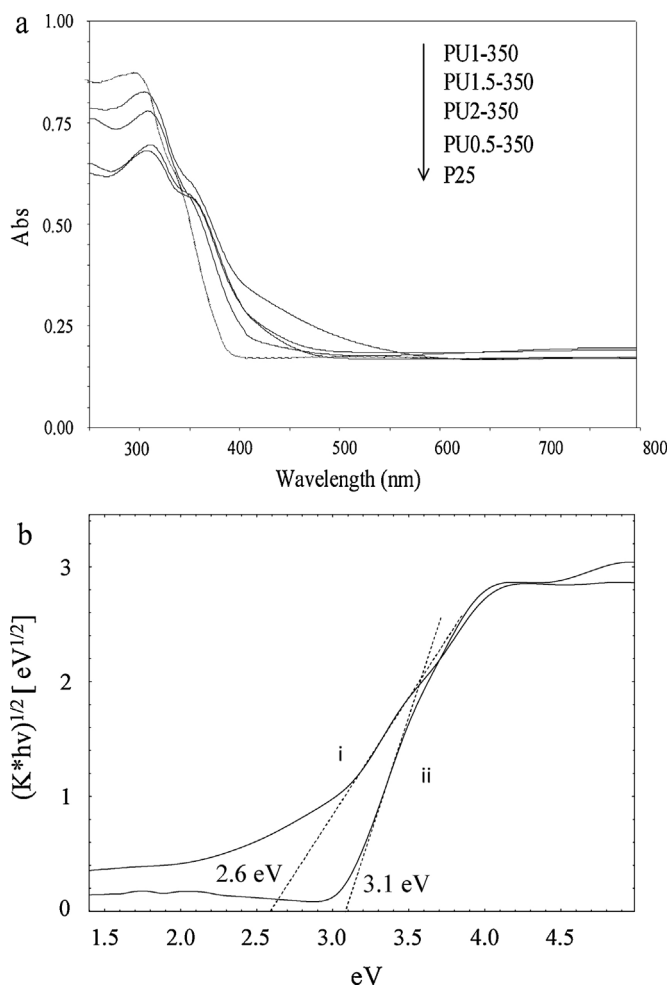


Fig. 4. UV-Vis diffused reflectance spectra of (a) pristine P25 and C coated N doped P25 samples and (b) plots of the transformed Kubelka-Munk function vs the energy of the light absorbed for PU1-350 (i) and pristine P25(ii).

for the standard anatase TiO_2 [27], while C coated N doped P25 has lower bandgap energies of ca. 2.6 eV. Due to the lower bandgap energy, this modified TiO_2 is expected to be visible light responsive.

3.1.4. XPS spectra

The chemical state and composition of the C coated N doped P25 at the surface were studied by XPS whose spectrum reveals the presence of Ti2p, O1s, C1s and N1s (see Fig. 5a-d) with the binding energy at 455, 526.5, 284.5 and 397.5 eV, respectively. As shown in Fig. 5a, XPS signals for Ti2p were observed at binding energies around 462.4 and 456.8 eV which as expected, confirmed the presence of $\text{Ti}2\text{p}_{1/2}$ and $\text{Ti}2\text{p}_{3/2}$, respectively [28]. Two minor peaks at 457.2 and 459.1 eV may be assigned to the presence of Ti-N-O and Ti-O-N, respectively [14]. The deconvolution of

O1s in Fig. 5b represented Ti-O and O-H bonds at 531.6 and 530.8 eV, respectively, [29,30] while the small peak at 533.4 eV was assigned as O-N [31]. In Fig. 5c, the deconvolutions of C1s peaks were observed at 284.5 and 283.9 eV which can be assigned to the adventitious element from the carbon tape used in the analysis and C-C bond from the carbon graphite bonding [32–34]. No peak was found around 282.6 to 282.9 eV that are normally associated with Ti-C [35] thus the possibility of C substitution doping was not observed in PU1-350 sample.

The binding energy for Ti-N was observed in the peak at 397.5 eV, as can be seen in Fig. 5d [36]. Therefore, XPS spectra

strengthened the evidence that C was just coated onto the surface of TiO_2 while N has a chemical bonding with the TiO_2 particle.

3.1.5. TEM and HRTEM

Fig. 6(a-d) shows the TEM and HRTEM images for pristine P25 and PU1-350 samples. TEM image confirmed the average particle size of the C coated N doped P25 to be within the range of 16 nm (Fig. 6b) and the size was more or less the same with the P25 particles (18 nm) as can be seen in Fig. 6a.

HRTEM was also used to estimate the thickness of C on the surface of TiO_2 -P25 particles. The image of Fig. 6c shows that the particle of P25 was coated with a thin layer of C with the fringe spacing similar to graphite at about 0.34 nm [37–39]. This confirmed the observed XPS results earlier that indicated the presence of the C graphite layer. The HRTEM image (Fig. 6d) also shows that the particle of P25 was completely surrounded with the C graphite layer. The coated C layer was observed to be about 2.04 nm. The thickness of the C layer is very important to the photocatalytic process since the thin layer of C is expected to allow better penetration of light to the surface of TiO_2 and should yield enhanced photocatalytic activity.

3.1.6. PL spectra

The photoluminescence (PL) spectroscopy was used to study the fate of electron–hole pairs in semiconductor particles since PL emission results from the recombination of charge carriers [39,40]. Fig. 7a and b shows the PL spectra of pristine P25 and various C coated N doped P25 samples at different heating temperatures using the excitation wavelength of 325 nm. It can be seen that all samples exhibit an obvious PL signal with a similar shaped curve at the wavelength range from 420 to 520 nm. The peak at 420 nm represents the band–band PL signal while the peak at 520 nm can be due to the excitonic PL signal originated mainly from the surface oxygen vacancies (O_v) and defects of semiconductors [40]. It was generally accepted that nitrogen doping can form a new electronic state (N state) just above the valence band, making TiO_2 to absorb visible light [41] and this was further confirmed experimentally by XPS valence band analysis (VB XPS), and visible light induced PL by Wu et al. [42].

From the density functional calculations (DFT), N-doping favored the formation of O_v , which was experimentally found to be about 0.8 eV below the bottom of the conduction band [42,43]. The O_v of nanosized semiconductor easily captures or bind with the photoinduced electrons [44] as proven by the electronic spin resonance method [45]. Hence, the larger the O_v content, the stronger the PL intensity. However, during the process of photocatalytic reaction, O_v and defects can become centers to capture photo-induced electrons, so that the recombination of photo-induced electrons and holes can be effectively inhibited [39]. Thus, it can be suggested that O_v and defects are in favor of photocatalytic reactions and the stronger the excitonic PL spectrum, the larger the content of O_v or defect, and the higher the photocatalytic activity.

The PL intensity of C coated, N doped P25 using 1 g urea at different temperatures are shown in Fig. 7a. Increasing excitonic PL intensity was detected when the temperature was increased up to 350 °C. However, the PL intensity decreased when the calcination temperature was increased beyond 350 °C. The decreasing PL intensity with increasing temperatures beyond 350 °C might be due to the decreasing doped N content [10] at higher calcination temperature as can be seen in Table 1 (column no 5). Thus the content of O_v formed decreased and less photo-induced electrons would be trapped by the O_v .

PL spectra for C coated N doped P25 samples with different amount of urea and calcined at 350 °C are shown in Fig. 7b. C coated N doped P25 samples showed higher PL intensity than pristine P25 where the sample with the highest amount of doped N possessing

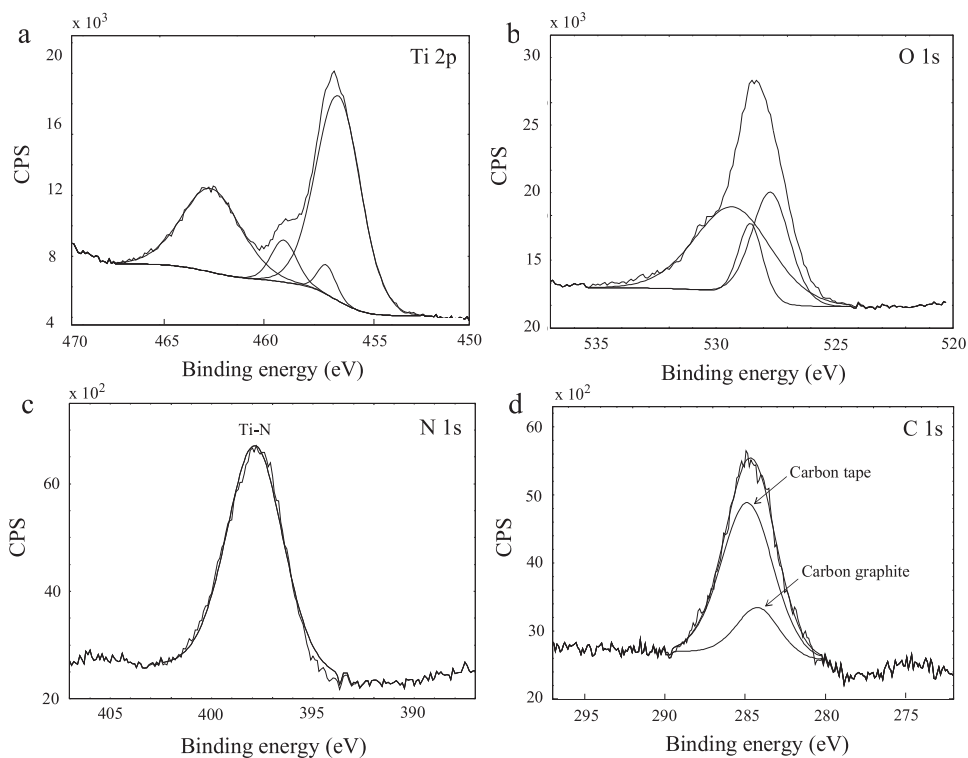


Fig. 5. XPS spectra of (a) the survey spectrum, (b) Ti 2p, (c) O 1s and (d) C 1s for the C coated N doped P25, PU1-350.

the highest PL intensity. The excitonic PL was increased by increasing the amount of doped N. However, the excitonic PL for PU1-350 was lower compared with the samples of PU0.5-350. This might be due to the presence of more C coated on the surface of TiO₂ in

PU1-350 than for PU0.5-350. Higher C coating can produce lower electron-hole recombination since C can function as electron scavenger as described by Janus et al. [46]. Therefore, two important phenomena occurred simultaneously in the C coated N doped P25:

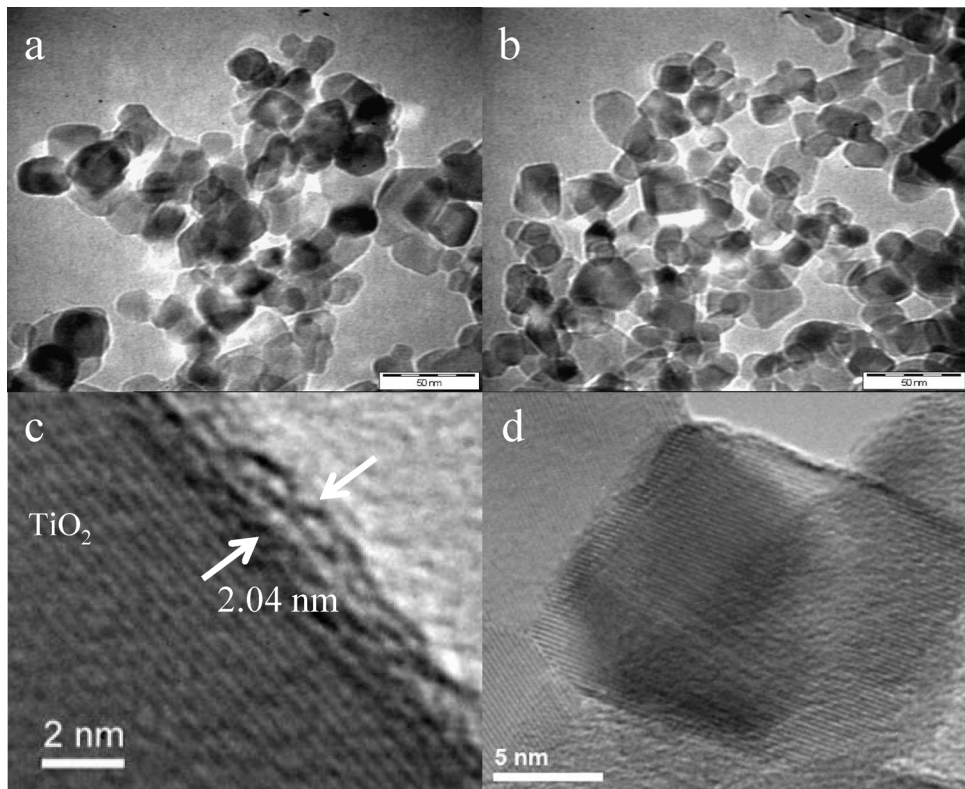


Fig. 6. TEM images of (a) P25 (b) PU1-350 while (c) and (d) are HRTEM images of PU1-350.

(1) Doping of N into P25 increases excitonic PL intensity due to increasing O_V and defect state of the photocatalyst and (2) coating of C onto P25 inhibits electron-hole recombination resulting in the decrease of the excitonic and band-band PL intensities [42]. On both occasions, the overall effect is to strongly inhibit the recombination of charge carriers within the photocatalyst.

3.1.7. Effect of aeration rate

All photocatalytic evaluations in this study were carried out under continuous aeration. Oxygen was found to be essential for the semiconductor photocatalytic degradation of organic contaminants [47]. Dissolved oxygen is usually employed as an electron acceptor [48]. The presence of an electron acceptor is essential in increasing the separation of the photogenerated electrons and holes, thus improving the efficiency of the photocatalytic process. In the aerated solution, the oxygen molecule is adsorbed onto the catalyst surface. The adsorbed oxygen molecules will be reduced to O₂^{•-} by electron that is promoted into the conduction band, leading to the formation of perhydroxyl radicals. In addition, perhydroxyl radical will produce hydrogen peroxide which can produce super hydroxyl radicals. The role of oxygen as an electron acceptor is summarized by the following equations [49]:



Fig. 8 shows the effect of flow rates towards photocatalytic degradation of RR4 dye using PU1-350 as the photocatalyst. It was found that 25 mL min⁻¹ was the optimum aeration rate where the degradation rate of RR4 was almost two times faster than the system running without aeration (stirring process). Therefore all photocatalytic and adsorption experiments in this work were carried out under this optimum aeration rate.

Photocatalytic degradation of RR4 dye using PU1-350 in the presence of nitrogen gas was also carried out in order to provide evidence for the role of O₂ in the photocatalytic process. It was found that the degradation rate of RR4 dye reduced significantly as compared to the experiment ran under aeration. This was due to the absence of the electron scavengers and the lack of the formation of superoxides. The role of superoxides in enhancing photocatalytic degradation of dyes was proven by running the experiment under aeration and in the presence of 1,4-benzoquinone, a known superoxide scavenger. Supplementary Fig. 1 clearly indicates that 1,4-benzoquinone significantly reduced the efficiency of the photocatalytic degradation of RR4 dye even though the solution was optimally aerated. Apparently superoxides produced via Eq.(1) was consumed by 1,4-benzoquinone thus making reactions 2–6 ceased to exist.

3.2. Effect of C and N contents

In this work, anionic RR4 dye was used as the model pollutant for optimizing the preparation of C coated N doped P25. The pseudo first order rate constants (K) for the degradation of RR4 using the 45-W compact fluorescent lamp without UV filter (source no 1: 3.5 W m⁻² of UV leakage) by various C coated N doped TiO₂-P25 samples under different calcining temperatures is presented in Fig. 9. The calcination of the catalyst at 350 and 400 °C produced significant photocatalytic activity where K values were higher compared with pristine P25. On the other hand, the catalyst prepared at

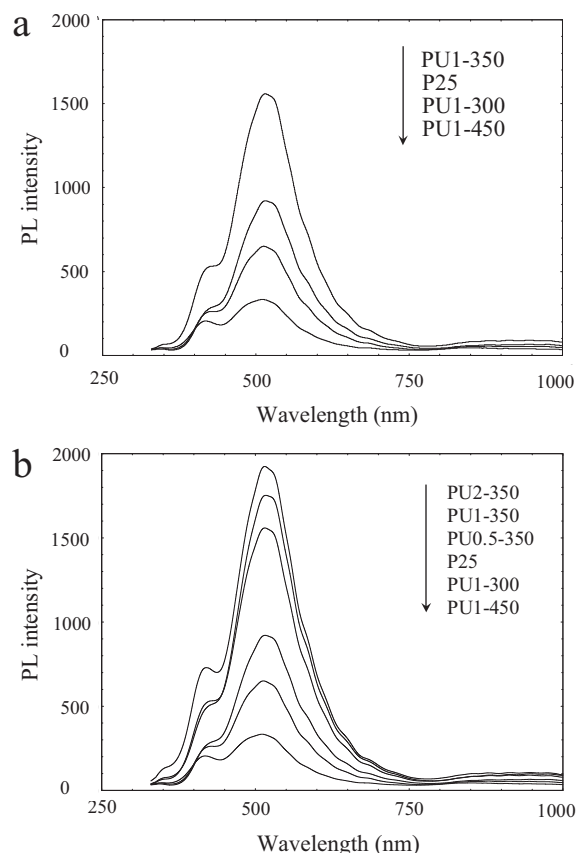


Fig. 7. Photoluminescence spectra of (a) pristine P25 and C coated N doped P25 at different calcination temperatures but similar amount of urea and (b) pristine P25 and C coated N doped P25 prepared at 350 °C containing different amount of urea.

calcinations temperature of 300, 450 and 500 °C became less effective. The trend for the K values was similar with the PL intensity in Fig. 7a where PU1-350 > P25 > PU1-300 > PU1-450. Beyond the calcining temperature of 350 °C, the photocatalytic efficiency of the products and also their respective PL intensity decreased due to the lesser production of O_V as described earlier. A similar trend was observed by Chen et al. [10] when they synthesized C, N co-doped TiO₂ via a sol-gel method at heating temperatures of 400 and 500 °C and applied the product to degrade MB under a visible light irradiation.

It was also observed that adding too much urea would also reduce the photocatalytic efficiency of the modified photocatalyst where the optimum TiO₂ to urea ratio was 3:1. The different K

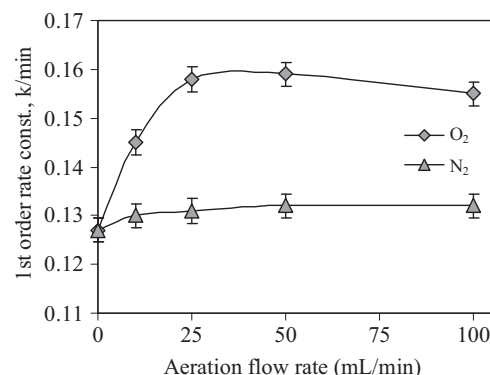


Fig. 8. Effect of aeration flow rates of air and nitrogen gas on the photocatalytic degradation of 30 mg L⁻¹ RR4 by PU1-350 under a 45-W fluorescent lamp.

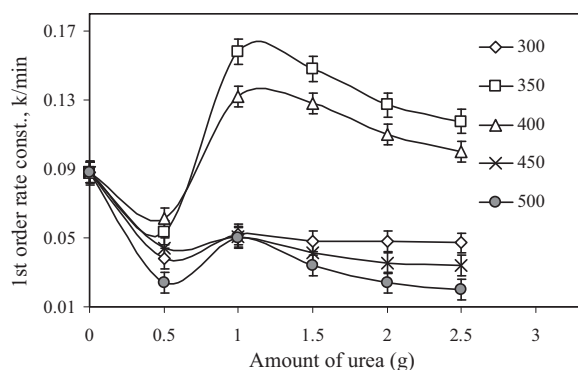


Fig. 9. Plots of the pseudo first order rate constants (K) for the degradation of 30 mg L^{-1} RR4 under 45-W fluorescent lamp for C coated N doped P25 samples prepared at different calcination temperatures and different amount of urea.

values observed for the RR4 degradation was due to the different amount of N and C incorporated into the TiO_2 -P25 crystal lattice. In one hand, N that was incorporated into the TiO_2 lattice could result in the band gap narrowing and red shift of absorption edge towards the visible-light region which increased its photocatalytic activity [36]. However when the N content is higher than the optimum amount, it could form high recombination centers [50,51] which eventually reduced its photocatalytic activity.

As can be seen in Fig. 10, pristine P25 adsorbed 30 mg L^{-1} RR4, 12.5 mg L^{-1} MB and 10 mg L^{-1} phenol by about 42, 11 and 7%, respectively, after 1 h of contact time. PU1-350 sample on the other hand, adsorbed c.a. 59, 11 and 8% of RR4, MB and phenol solutions, respectively. Pristine TiO_2 -P25 and PU1-350 has a strong adsorption for anionic RR4 dye due to the coulombic attraction by the positively charged pristine P25 and PU1-350. This is proven via the measurement of zeta potentials of these photocatalysts at ambient condition (pH 5.5). The zeta potential of pristine P25 was observed to be 0.79 mV while the zeta potential for PU1-350 was 15.57 mV . This explains why PU1-350 adsorbed anionic RR4 dye better than pristine P25 despite of its lower surface area. The adsorption was less for MB and phenol due to the repulsion that occurs between the positively charged MB and non-charged phenol (at ambient pH) against the positively charged catalyst particles.

During the removal of pollutants under light irradiation, two processes occurred simultaneously namely adsorptive and photocatalytic processes. In order to minimize the effect of the physical adsorption and to make the photocatalytic process dominant, a study was also done whereby the samples were first pre-saturated with the respective pollutants prior to switching on the light for photocatalysis. In this way, it was assumed that only photocatalytic process occurred in the removal of the pollutants. Fig. 11

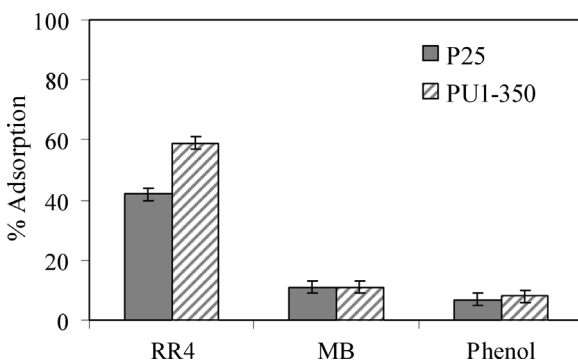


Fig. 10. Adsorption study of pristine P25 and PU1-350 under RR4, MB and phenol.

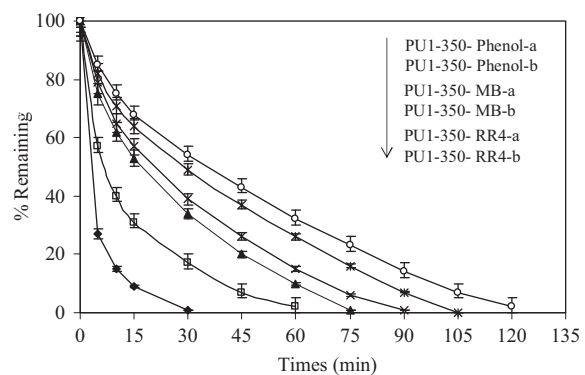


Fig. 11. Plots of the photocatalytic degradation of pollutants using (a) pre-saturated PU1-350 with individual pollutant and (b) unsaturated PU1-350 both under 45-W fluorescent lamp.

shows the removal of pollutants (RR4, MB and phenol) under pre-saturated PU1-350 and unsaturated PU1-350 samples. The degradation of RR4, MB and phenol was always better when both processes occurred simultaneously(adsorption + photocatalytic) as compared to the isolated photocatalytic process only.

3.3. Effect of different light irradiations

The 45-W compact fluorescent lamp had a residual UV irradiance leakage of 3.5 W m^{-2} . The UV irradiation becomes zero (0.0 W m^{-2}) when the UV filter was attached to the 45-W fluorescent lamp while the visible light reading recorded was 265 W m^{-2} . Fig. 12a shows the photocatalytic degradation of RR4 dye by PU1-350 and pristine P25 under the 45-W fluorescent lamp (UV-Vis). It was found that PU1-350 took only 30 min to complete the RR4 degradation as compared with pristine P25 that needed longer irradiation time to complete the same degradation process. The pseudo first order rate constant K values for the degradation of RR4 by PU1-350 was about 1.8 times faster than pristine P25 where the values were 0.158 and 0.088 min^{-1} , respectively. High photocatalytic activity of PU1-350 was due to the presence of C as the electron scavenger that reduced the electron-hole recombination during the photocatalytic process as previously confirmed by the lowest PL intensity of PU1-350 sample as well as its ability to utilize visible light component of the light source. Similar observation was reported by Janus et al. [46] where the C coated on the TiO_2 surface photoaccelerated the process by acting as the electron scavenger.

The photocatalytic degradation of RR4 under visible light irradiation was also displayed in Fig. 12a (UV-filter). Pristine P25 was observed to degrade RR4 dye by about 42% but no further degradation was observed beyond that level even after prolonged irradiation. In fact the removal of RR4 dye by pristine TiO_2 here was mainly from the adsorption process where no photocatalytic reaction actually occurred as indicated in Fig. 10. Similar observation (no photocatalytic degradation) was also observed when pristine P25 was applied for the degradation of MB (Fig. 12b) and phenol (Fig. 12c) under visible light irradiation. However, photocatalytic activity was observed when PU1-350 was irradiated under visible light irradiation (UV-filter) where it completed the degradation of RR4 within 45 min of contact time. PU1-350 had also degraded MB and phenol under visible light irradiation as can be seen in Fig. 12b and c. These results clearly proved that the band gap energy of PU1-350 was red shifted due to the mixing of N 2p and O 2p states [3,16] thus allowing it to function under visible light. The calculation of the electronic state of N-doped TiO_2 by Chamber et al. [52] indicated that there was virtually no shift of the valence band by mixing the N 2p and O 2p states within the N-doped TiO_2 . However, they found that the N impurity level appeared slightly above the valence band

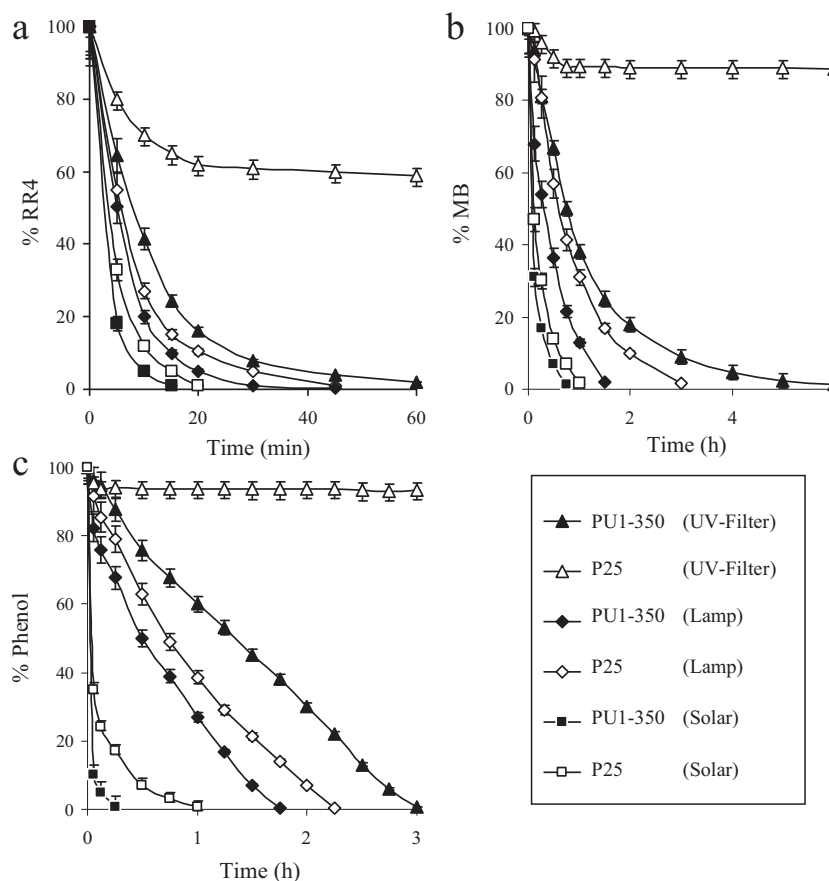


Fig. 12. The effect of different light sources on the photocatalytic activities of the pristine P25 and PU1-350 photocatalysts in the degradation of (a) 30 mg L^{-1} RR4, (b) 12 mg L^{-1} MB (b) and (c) 10 mg L^{-1} phenol solution under 45-W fluorescent lamp and (a) 60 mg L^{-1} RR4, b) 36 mg L^{-1} MB (b) and (c) 30 mg L^{-1} phenol solution under solar irradiation.

($\sim 0.8 \text{ eV}$). This is in agreement with our XPS results shown in Fig. 5c where it shows that N was incorporated into TiO_2 lattice by replacing an O atom. It is therefore suggested that an isolated N impurity level above the valence band in PU1-350 may be responsible for the visible light absorption.

Solar light which contains about 5% UV radiation [53] (22 W m^{-2} in this study) should produce excellent photocatalytic activity of the samples. As shown in Fig. 12a–c, a complete degradation of 60, 36 and 30 mg L^{-1} of RR4, MB and phenol by PU1-350 sample under solar irradiation took only 20, 15 and 15 min, respectively, compared to pristine P25 which took 30, 45 and 30 min using the same pollutants. It can be summarized that C coated N doped P25 was faster by 2 times than the pristine TiO_2 -P25 in the photocatalytic degradation of RR4, MB and phenol, respectively, under solar irradiation. Therefore this study proved that thin C coated N doped P25 has a great potential to be used for solar detoxification of organic pollutants.

3.4. Mineralization study

Mineralization is defined as the complete decomposition of organic compounds into CO_2 and H_2O . Achieving a complete mineralization should therefore be the target of any photocatalytic processes. The degree of mineralization can be indicated by monitoring the total organic carbon (TOC) values of the treated samples. TOC is considered the most relevant for the determination of organic pollution. The TOC values of phenol, MB and RR4 samples after photocatalytic treatment with both pristine P25 and PU1-350 samples are given in Fig. 13. The percentages of mineralization

achieved by PU1-350 were much higher than that of the pristine TiO_2 -P25. For PU1-350, complete mineralization of RR4, MB and phenol was achieved after 5, 7 and 7 h of irradiation, respectively, using the compact 45 W fluorescent light source. For pristine TiO_2 -P25 sample, the remaining TOC values were still significantly higher at 47, 40 and 34%, respectively, for RR4, MB and phenol under the same conditions.

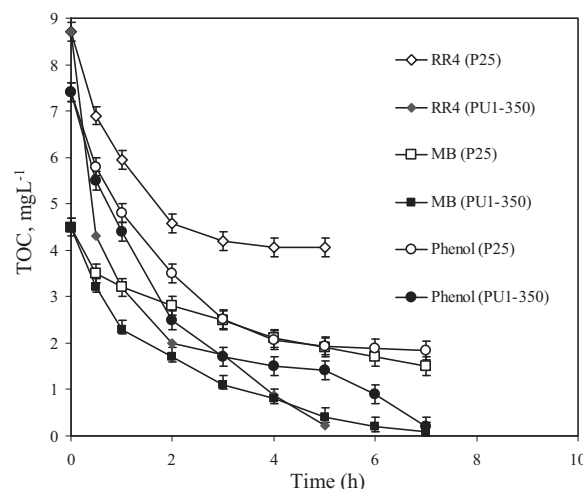


Fig. 13. Mineralization process of RR4, MB and phenol of pristine P25 and PU1-350 under 45-W fluorescent lamp.

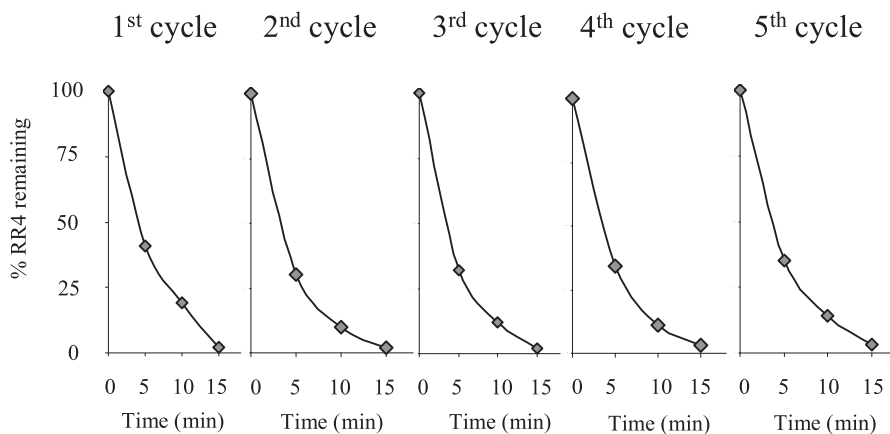


Fig. 14. Photocatalytic efficiency of PU1-350, C coated N doped P25 upon recycled applications in the degradation of RR4 dye irradiated under a 45 W fluorescent lamp.

Table 3

Carbon content of C coated N doped TiO₂-P25 upon prolonged irradiations with a 45 W fluorescent lamp in distilled water for 0, 24, 48 and 72 h.

Irradiation times (h)	0	24	48	72
Carbon content (%)	1.39 (± 0.03)	1.35 (± 0.03)	1.35 (± 0.03)	1.32 (± 0.03)
Nitrogen content (%)	2.27 (± 0.03)	2.24 (± 0.03)	2.24 (± 0.03)	2.22 (± 0.03)

3.5. The stability of the photocatalyst

For the stability study of the photocatalyst, the suspended PU1-350 particles in ultrapure water were exposed to the 45 W fluorescent lamp irradiation for 24, 48 and 72 h, respectively. Table 3 shows the amount of N and C content of PU1-350 under prolonged irradiation times. The result shows that the N and C content of the irradiated.

PU1-350 particles remained constant even up to 72 h of direct irradiation. Fig. 14 shows the result of the repeated reuse or recycling of the PU1-350 photocatalyst for the degradation of RR4 dye upon 15 min of irradiation time. It was observed that each time of recycled application produced 97.6 ± 0.6% removal of RR4 indicating a sustainable photocatalytic efficiency characteristic. In other words, a strong interaction of C with P25 occurred due to its strong chemisorption on the surface of TiO₂ where it was not easily removed even after 5 times of repeated usage.

4. Conclusion

A visible light active C coated N doped P25 photocatalyst was successfully prepared via controlled doping of urea into P25 powder under a relatively low temperature heating process. It was observed that utilization of 3:1 P25 to urea ratio with 350 °C calcination temperature produced C coated N doped P25 with optimum photocatalytic activity. The treatment process however caused a reduction of BET surface areas of the photocatalyst but did not produce any phase transformation even at 500 °C. From the HRTEM image, it was observed that a thin C graphite layer of 2.04 nm was coated onto the surface of P-25 particles. XPS analysis confirms that the modified photocatalyst possessed N which substitutes the oxygen molecules to produce Ti–N at binding energy of 395.7 eV. The bandgap energy of the C coated N doped P25 was 2.6 eV as seen from its UV–Vis DRS spectrum. The enhancement of the photocatalytic efficiency was postulated to be due to the significant reduction of the e[−]h⁺ recombination, as indicated by the high excitonic PL signal intensity for the optimum PU1-350 sample. Moreover, the presence of doped N makes PU1-350 to be active under visible light irradiation. The efficiency of the modified catalyst was 1.8 times better

than P25 under visible light fluorescent lamp and 2 times better under solar irradiation. Finally, C coated N doped P25 was very stable and possessed excellent sustainable photocatalytic activity with no loss of C and N detected even after 5 times of reuse.

Acknowledgements

We would like to thank the Malaysian Ministry of Science and Technology (MOSTE) for providing generous financial support under Scifund and FRGS grants to conduct this study and Universiti Sains Malaysia for providing all the needed facilities.

Appendix A. Supplementary data

Supplementary data associated with this article can be found, in the online version, at <http://dx.doi.org/10.1016/j.molcata.2013.11.030>.

References

- [1] M.R. Hoffmann, S.T. Martin, W. Choi, D.W. Bahnemann, Chem. Rev. 95 (1995) 69–96.
- [2] A. Kudo, K. Omori, H. Kato, J. Am. Chem. Soc. 121 (1999) 11459.
- [3] R. Asahi, T. Morikawa, T. Ohwaki, K. Aoki, Y. Taga, Science 293 (2001) 269–271.
- [4] Y. Park, W. Kim, H. Park, T. Tachikawa, T. Majima, W. Choi, Appl. Catal., B: Environ. 91 (2009) 355–361.
- [5] G.T. Lim, K.H. Kim, J. Park, S-H. Ohk, J-H. Kim, D.L. Cho, J. Ind. Eng. Chem. 16 (2010) 723–727.
- [6] C. Han, M. Pelaez, V. Likodimos, A.G. Kontos, P. Falaras, K. O'Shea, D.D. Dionysiou, Appl. Catal., B: Environ. 107 (2011) 77–87.
- [7] H. Sun, H. Liu, J. Ma, X. Wang, B. Wang, L. Han, J. Hazard. Mater. 156 (2008) 552–559.
- [8] N. Todorova, T. Giannakopoulou, T. Vaimakis, C. Trapalis, Mater. Sci. Eng. B 152 (2008) 50–54.
- [9] C. He, D. Shu, M. Su, D. Xia, M.A. Asi, L. Lin, Y. Xiong, Desalination 253 (2010) 88–93.
- [10] D. Chen, Z. Jiang, J. Geng, Q. Wang, D. Yang, Ind. Eng. Chem. Res. 46 (2007) 2741–2746.
- [11] A. Roguska, A. Kudelski, M. Pisarek, M. Opara, M.J. Czachor, Appl. Surf. Sci. 257 (2011) 8182–8189.
- [12] L. Tao, Z. Zhu, F. Li, Colloids Surf., A 425 (2013) 92–98.
- [13] T. Morikawa, T. Ohwaki, K. Suzuki, S. Moribe, S.T. Kubota, Appl. Catal., B: Environ. 83 (2008) 56–62.
- [14] F. Li, Y. Zhao, Y. Hao, X. Wang, R. Liu, D. Zhao, D. Chen, J. Hazard. Mater. 239 (2012) 118–127.
- [15] P. Wang, T. Zhao, R. Wang, T.T. Lim, Water Res. 45 (2011) 5015–5026.
- [16] J.A.R. Herrera, J. Kiwi, C. Pulgarin, J. Photochem. Photobiol., A 205 (2009) 109–115.
- [17] T. Tsumura, N. Kojitani, I. Izumi, N. Iwashita, M. Toyoda, M. Inagaki, J. Mater. Chem. 12 (2002) 1391–1396.
- [18] J.H. Park, S. Kim, A.J. Bard, Nano Lett. 6 (2006) 24–28.
- [19] S. Sato, R. Nakamura, S. Abe, Appl. Catal., A: Gen. 284 (2005) 131–137.
- [20] A. Fujishima, K. Honda, Nature 238 (1972) 37–38.
- [21] A. Zaleska, Recent Pat. Eng. 2 (2008) 157–164.

- [22] Y.C. Hsu, H.C. Lin, C.W. Lue, Y.T. Liao, C.M. Yang, *Appl. Catal., B: Environ.* 89 (2009) 309–314.
- [23] J. Zhang, Z. Huang, Y. Xu, F. Kang, *New Carbon Mater.* 26 (2011) 63–70.
- [24] B. Tryba, A.W. Morawski, T. Tsumura, M. Toyoda, M. Inagaki, *J. Photochem. Photobiol., A* 167 (2004) 127–135.
- [25] H. Zhang, J.F. Banfield, *J. Phys. Chem. B* 104 (2000) 3481–3487.
- [26] R. Nakamura, T. Tanaka, Y. Nakato, *J. Phys. B* 108 (2004) 10617.
- [27] C. Shifu, L. Yunzhang, *Chemosphere* 67 (2007) 1010–1017.
- [28] M. Xing, J. Zhang, F. Chen, *Appl. Catal., B: Environ.* 89 (2009) 563–569.
- [29] Q. Xu, D.V. Wellia, M.A. Sk, K.H. Lim, J.S.C. Loo, D.W. Liao, R. Amal, T.T.Y. Tan, *J. Photochem. Photobiol., A* 210 (2010) 181–187.
- [30] L. Ge, M. Xu, H. Fang, *Thin Solid Films* 515 (2007) 3414–3420.
- [31] F. Meng, Z.L. Hong, J. Amdt, M. Li, M.J. Zhi, F. Yang, N.Q. Wu, *Nano Res.* 5 (2012) 213–221.
- [32] X. Chen, P. Glans, X. Qiu, S. Dayal, W.D. Jennings, K.E. Smith, C. Burda, J. Guo, *J. Electron. Spectrosc. Relat. Phenom.* 162 (2008) 67–73.
- [33] F. Jia, Z. Yao, Z. Jiang, C.X. Li, *Catal. Commun.* 12 (2011) 497–501.
- [34] Q. Xiao, J. Zhang, C. Xiao, Z. Si, X. Tan, *Sol. Energy* 82 (2008) 706–713.
- [35] S.M. Yun, K. Palanivelu, Y.H. Kim, P.H. Kang, Y.S. Lee, *J. Ind. Eng. Chem.* 14 (2008) 667–671.
- [36] L. Mi, P. Xu, H. Shen, P.N. Wang, *J. Photochem. Photobiol., A* 193 (2008) 222–227.
- [37] L.W. Zhang, H.B. Fu, Y.F. Zhu, *Adv. Funct. Mater.* 18 (2008) 2180–2189.
- [38] Y. Wang, R. Shi, J. Lin, Y. Zhu, *Appl. Catal., B: Environ.* 100 (2010) 179–183.
- [39] M. Inagaki, *Carbon* 50 (2012) 3247–3266.
- [40] J.M. Timothy, *Ultrason. Sonochem.* 10 (2003) 175–179.
- [41] S. Livraghi, M.C. Paganini, E. Giamello, A. Selloni, C. DiValentin, G. Pacchioni, *J. Am. Chem. Soc.* 128 (2006) 15666–15671.
- [42] Z. Wu, F. Dong, W. Zhao, S. Guo, J. Hazard. Mater. 157 (2008) 57–63.
- [43] M.A. Henderson, W.S. Epling, C.H.F. Peden, C.L. Perkins, *J. Phys. Chem. B* 107 (2003) 534–545.
- [44] L.Q. Jing, B.F. Xin, F.L. Yuan, L.P. Xue, B.X. Wang, H.G. Fu, *J. Phys. Chem. B* 110 (2006) 17860–17865.
- [45] L.Q. Jing, Z.L. Xu, X.J. Sun, J. Shang, W.M. Cai, *Appl. Surf. Sci.* 180 (2001) 308–314.
- [46] M. Janus, M. Inagaki, B. Tryba, M. Toyoda, A.W. Morawski, *Appl. Catal., B: Environ.* 63 (2006) 272–276.
- [47] O. Carp, C. L. Huisman, A. Reller, *Prog Solid State Chem.* 32 (2004) 33–177.
- [48] M.N. Chong, B. Jin, C.W.K. Chow, C. Saint, *Water Res.* 44 (2010) 2997–3027.
- [49] K.H. Wang, Y.H. Hsieh, P.W. Chao, C.Y. Cgang, J. Hazard. Mater. 95 (2002) 161–174.
- [50] G. Liu, X. Wang, L. Wang, Z. Chen, F. Li, H.M. Gao Qin, J. Cheng, *Colloid Interface Sci.* 334 (2009) 171–175.
- [51] G. Liu, X. Wang, Z. Chen, H.M. Cheng, G.Q. Lu, *J. Colloid Interface Sci.* 329 (2009) 331–338.
- [52] S.A. Chamber, S.H. Cheung, V. Shutthanandan, S. Thevuthasan, M.K. Bowman, A.G. Joly, *Chem. Phys.* 339 (2007) 27–35.
- [53] R.P. Sinha, M. Klisch, A. Vaishampayan, D.P. Hader, *Acta Protozoologica* 38 (1999) 273–290.